

observed in the negative ion LMS spectra of Ba and Pb complexes (Table III).

Evidence for processes corresponding to ion-molecule reactions is also observed in the negative ion LMS spectra of the complexes. For example, the negative ion LMS spectra of $[M(o\text{-phen})_3]Cl_2$ ($M = Co, Ni$) shows ions corresponding to MCl_2CN^- , MCl_2^- , C_3N^- , Cl^- , and CN^- (Table III); CN^- ions produced in the plasma react to yield mixed cluster ions. Similar species involving CN^- ions are also observed in the negative ion LMS spectrum of $[Cu(dmp)_2]_2SO_4 \cdot 5H_2O$ (Table III).

In short, the negative ion spectra are useful for obtaining information about the anions, other anions produced by ion-molecule reactions, and the oxidation state of the central metal ion of the complex; they also provide supporting evidence for internal decomposition.

Acknowledgment. We are grateful to Professor B. E. Douglas and Dr. S. K. Viswanadham for useful discussions. Support of this work by the Office of Naval Research is gratefully acknowledged.

Contribution from the Department of Chemistry,
Yale University, New Haven, Connecticut 06511

Paramagnetic Phosphine Shift Reagents. 2. Study of the Structures of (Substituted-allyl)palladium Complexes in Solution

J. W. Faller,* C. Blankenship, B. Whitmore, and S. Sena

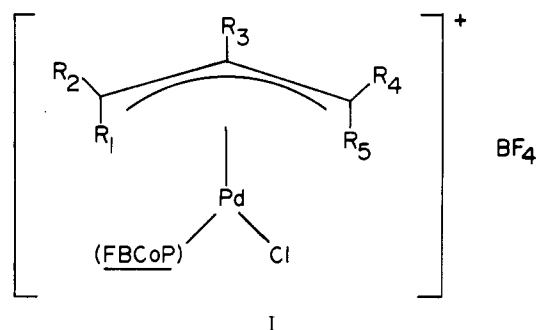
Received December 5, 1984

The use of a paramagnetic shift reagent analogue of a phosphine ligand for elucidation of the structures of (substituted-allyl)palladium complexes is described. Deuterium quadrupole splittings and isotropic shifts can be predicted from geometrical parameters based on model compounds. The magnetic susceptibility anisotropy is effectively constant within a series of complexes and allows predictions of shifts and/or geometry. Fitting of the data for a (η^3 -2-methylallyl)Pd complex required that the terminal protons be twisted out of the plane of the allyl carbon atoms. This twisting was confirmed by X-ray crystallographic analysis of a model compound, (η^3 -2-methylallyl)PdCl[P(C₆H₅)₃]. Crystal data: space group $P2_1/c$; $a = 11.931$ (4) Å; $b = 9.783$ (2) Å; $c = 17.286$ (6) Å; $\beta = 97.40$ (3)°; $V = 2001$ (2) Å³; $M_r = 459.25$; $Z = 4$; $\rho_{\text{calcd}} = 1.53$ g/cm³. For 2219 reflections ($F^2 \geq 3.0\sigma(F^2)$), $R_1 = 0.036$ and $R_2 = 0.040$.

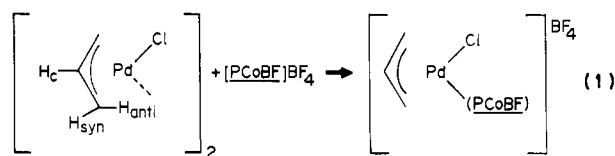
Paramagnetic shift reagents have been extensively studied with respect to the probing of geometry and conformation of substrates in solution.¹ Conventional reagents, such as lanthanide shift reagents, utilize the Lewis base affinity of metal ions for binding of substrates.² We recently reported³ the use of a shift reagent that possesses a phosphorus donor site capable of binding to Lewis acid centers and thereby allowing one to probe the structure of analogues of transition-metal complexes in solution. The exploitation of complexes that can be used as shift reagents, such as $[PCoBF]BF_4$ (see Figure 1), first prepared by Holm's group,^{4,5} is desirable owing to the ubiquitous presence of phosphine ligands in organometallics and the need to develop structural probes capable of characterizing catalytic intermediates in solution. We now report the synthesis and spectral characterization of a series of (substituted-allyl)palladium complexes of the general form shown in I.

Results and Discussion

The paramagnetic phosphine ligand is introduced into the palladium complex via the bridge-splitting reactions of the allylpalladium halide dimers (eq 1). The resulting palladium



- 1, $R_1 - R_5 = H$
 2, $R_1 = R_2 = R_3 = R_4 = H, R_5 = CH_3$
 3, $R_1 = R_2 = R_3 = R_5 = H, R_4 = CH_3$
 4, $R_1 = R_2 = R_3 = H, R_4 = R_5 = CH_3$
 5, $R_1 = R_3 = R_5 = H, R_2 = R_4 = CH_3$
 6a, $R_1 = R_2 = R_5 = H, R_3 = CH_3, R_4 = COCH_3$
 6b, $R_1 = R_2 = R_4 = H, R_3 = CH_3, R_5 = COCH_3$



- (1) Orrell, K. G. *Annu. Rep. NMR Spectrosc.* **1979**, *10*, 1 and references therein.
 (2) LaMar, G. N., Horrocks, W. D., Jr., Holm, R. H., Eds. "NMR of Paramagnetic Molecules"; Academic Press: New York, 1973.
 (3) Faller, J. W.; Blankenship, C.; Sena, S. *J. Am. Chem. Soc.* **1984**, *106*, 793-795.
 (4) Parks, J. E.; Wagner, B. E.; Holm, R. H. *Inorg. Chem.* **1971**, *10*, 2472-2478.
 (5) Larsen, E.; LaMar, G. N.; Wagner, B. E.; Parks, J. E.; Holm, R. H. *Inorg. Chem.* **1972**, *11*, 2652-2667.

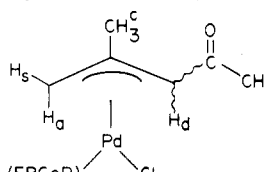
complexes are all isolated as yellow air-stable solids, but undergo gradual decomposition in solution over several days. In the ¹H NMR spectra of the [(allyl)Pd(PCoBF)]BF₄ complexes, one observes that the resonances of the allylic ligands are shifted far downfield from the positions in their analogous diamagnetic dimers and triphenylphosphine complexes, as summarized in Tables I-III.

Assignment of Resonances. The resonances are assigned on the basis of their estimated relative distances and angles from the

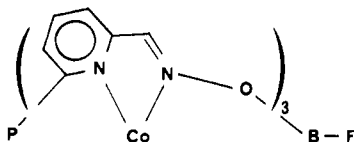
Table I. 270-MHz ¹H NMR Spectral Data for [(allyl)Pd(*PCoBF*)]BF₄ Complexes

complex ^c	25 °C					-50 °C				
	δ ₁	δ ₂	δ ₃	δ ₄	δ ₅	δ ₁	δ ₂	δ ₃	δ ₄	δ ₅
1	32.5 (28.8)	35.7 (31.0)	26.5 (20.2)	22.9 (17.8)	25.3 ^a (21.0)	49.9	55.1	38.6	32.9	37.4
2, 2-Me^b	32.0 (28.3)	34.6 (29.9)	17.8 (15.7)	22.7 (17.7)	25.3 ^a (21.2)	48.1	52.2	26.6	32.4	37.2
3, 1-Me^b	32.5	35.7	26.2	14.0	26.2	49.6	54.9	38.1	20.9	37.9
4, 1,1-Me^b	32.3	34.9	26.2	14.0	17.6	48.5	52.6	37.7	21.0	26.5
5, 1,3-Me^b	32.7	22.0	26.0	13.9	25.8	49.1	34.2	37.1	20.6	37.1

^a Allyl resonance obscured by a *PCoBF* ligand resonance. ^b Methyl group resonances are indicated in boldface type. ^c Values in parentheses are Δδ, the difference shifts with respect to the analogous zinc complex. ^d Resonances due to the *PCoBF* ligands were observed in the following ranges at 25 °C: δ 25.2–25.6, 101.6–101.9, 123.3–124.2. At -50 °C only one resonance at δ 23.6–24.6 was observed, the other two being broad and having shifts greater than δ 130.

Table II. 270-MHz ¹H NMR Spectral Data for [(1-acetyl-2-methylallyl)Pd(*PCoBF*)]BF₄


proton	25 °C		-50 °C	
	A 52%	B 48%	A 55%	B 45%
H _a	34.4	32.4	48.6	49.3
H _b	35.6	34.4	53.7	52.9
Me _c	18.4	18.1	27.7	27.4
H _d	26.6	24.2	38.8	34.6
Me _e	13.0	13.7	19.2	20.4

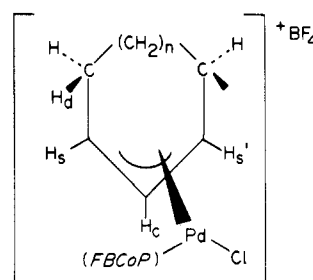
**Figure 1.** Structure of the clathrochelate cation used as a shift reagent in these studies. This structure is indicated as *PCoBF* for the Co²⁺ derivative. The diamagnetic Zn²⁺ analogue is designated as *PZnBF*.

paramagnetic cobalt(II) center in the phosphine ligand [*PCoBF*]⁺BF₄⁻ and by observed differences in spectra between complexes containing methyl groups in various positions on the allyl. The isotropic shifts of the protons are related to the geometrical parameters relative to the cobalt(II) according to eq 2, where *r* is

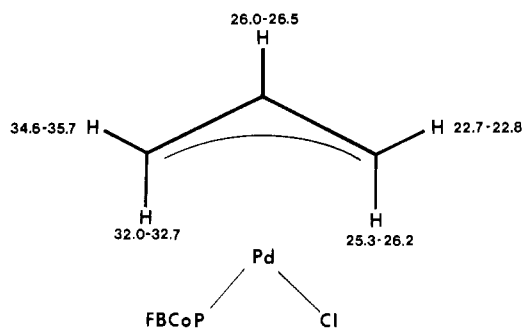
$$\Delta H/H = D(3 \cos^2 \theta - 1)/r^3 \quad (2)$$

the Co–H distance, θ is the angle between the Co–H vector and the Co–P vector, and *D* is a constant containing magnetic susceptibility terms. Since the *D* factor is temperature-dependent, the dipolar shifts of different compounds should be compared at the same temperatures.

Through comparison of the allyl and 2-methylallyl complexes one notes that the resonance at $\delta \sim 26$ (25 °C) can be assigned to the central allylic position, as the other resonances show very little shift, and the methyl resonance can be readily identified by its 3:1 intensity ratio. Due to their proximity to the Co atom, the two most shifted resonances can be assigned to the *syn* and *anti* protons cis to the *PCoBF* ligand. However, models based on crystal structures can not be used here to clearly differentiate between the two. If one assumes that the replacement of *syn* hydrogen by a methyl group does not produce a significant distortion of the H_{anti} orientation, reference to the *syn,syn*-1,3-dimethylallyl complex⁶ (**5**) allows the following assignments at 25 °C: H_a, δ 32.0–32.7; H_b, δ 34.6–35.7; H_c, δ 22.7–22.8; and H_d,

Table III. 270-MHz ¹H NMR Spectral Data for [(cyclic allyl)Pd(*PCoBF*)]BF₄ Complexes at -50 °C


proton	cyclohexenyl (n = 1)	cycloheptenyl (n = 2)
H _a	51.3	49.6
H _b	43.3	42.0
H _c	39.4	38.2
		36.86
H _s	33.98	34.08
	30.56	
	27.19	28.20
	25.49	24.12
<i>PCoBF</i>	23.85	23.83
	21.17	23.37
	20.22	21.76
		19.78
		19.54

**Figure 2.** Ranges for ¹H chemical shifts in type I complexes.

δ 25.3–26.2. The greater shift of H_a relative to H_c is readily predicted from models.

Applications to Isomer Identification. The allyl resonances that are replaced by upfield methyl resonances in **3** and **4** clearly demonstrate that the methyl-substituted termini are *trans* to the phosphine ligand, as previously postulated for the triphenylphosphine analogue of complex **4**.⁷

Another complex which clearly can be shown to have the *trans* geometry with an acetyl substituent *trans* to the phosphine is [(1-acetyl-2-methylallyl)PdCl(*PCoBF*)]BF₄ (**6**). The ¹H NMR spectral data in Table II clearly show the presence of only two isomers, which both have an acetyl *trans* to *PCoBF* but differ by

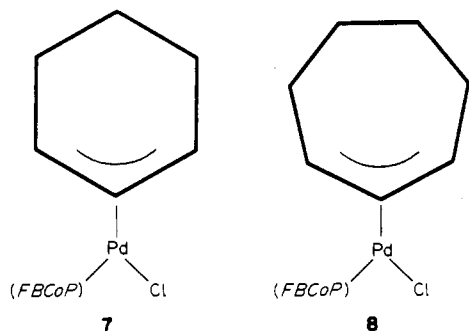
(6) Faller, J. W.; Thomsen, M. E.; Mattina, M. J. *J. Am. Chem. Soc.* **1971**, *93*, 2642–2653.

(7) Mason, R.; Russell, D. R. *Chem. Commun.* **1966**, 26.

having syn and anti acetyl groups. For analogous complexes with pyridine ligands, only the trans isomers are observed,⁶ consistent with the assignment made here. The observed chemical shifts for the acetyl methyl groups are similar to those for the methyl groups in the trans-methyl-substituted allyl complexes (see Table I). If one or both of the isomers contained a cis-acetyl group, a spectrum with more highly shifted methyl groups would be expected. One would also observe a methyl absorption further downfield as is observed for the cis methyl in [(1,3-dimethylallyl)PdCl(PCoBF)]BF₄. In contrast to complexes 3 and 5 where the syn isomers predominate, the acetyl group in complex 6 is present in both syn and anti orientations. The ratio of isomers in 6 is nearly 1:1; a 48:52 ratio is observed at 25 °C and a 45:55 ratio is seen at -50 °C based on integration of the acetyl methyl resonances and the proton of the allyl fragment α to the carbonyl ligand, H_d.

The relative positions of these two types of protons, H_{d-syn} and H_{d-anti}, in the different isomers allow the assignment of each set of resonances to the appropriate isomer. Thus, the set of resonances having H_d at lowest field, i.e. an anti proton (δ 38.8 at -50 °C), is assigned to the syn-acetyl isomer, 6s. The relatively facile equilibrium between syn and anti acetyl complexes is easily shifted and is a sensitive function of the ligand. Thus, in (1-acetyl-2-methylallyl)PdCl(pyridine), the anti acetyl isomer is favored by a 3:1 margin over the syn isomer.⁶ In the absence of a central substituent the syn isomer dominates (>94%), but steric interactions with a central substituent destabilize this orientation and an anti isomer can become preferred. Steric interactions with the ligand also modify the stability, and the equilibrium constant can be tuned by these factors. There also appears to be the possibility that in the anti isomer the acetyl group may weakly bind to the palladium. The proton spectrum does not provide enough information to examine this possibility; however, we are examining the NMR spectra of other nuclei to investigate the situation.

Applications to Cyclic Allyls. The results of the examination of ¹H NMR spectra of the cyclohexenyl (7) and cycloheptenyl (8) palladium complexes are summarized in Table III. Owing



to the complexity of the spectra, full assignments of the resonances were not carried out. However, through comparison of resonances for 7 and 8 with those of 1-6 a partial assignment is straightforward. The presence of a cyclic allyl ligand requires the methylenes to assume anti orientations and thus place the terminal protons of the allyl into syn positions. These are readily assigned to the cis and trans protons, H_s and H_{s'}, at δ 51.3 and 33.98 for 7 and δ 49.6 and 34.08 for 8. The assignment of the central proton, H_c, at δ 39.4 and 38.2 is also straightforward. Most other assignments would be tentative at this point; however, H_d, owing to its proximity to the Co ion, would be expected to show an extremely large shift. Thus, the resonances at δ 43.3 and 42.0 are assigned to this α proton, H_d, in 7 and 8.

This is a much greater shift than would be observed for a methyl group in a comparable position, since the proton is held close to the Co(II) rather than experiencing an averaged environment both near the metal and removed from the metal. We are currently examining the ¹³C NMR spectra to examine the practicality of determining ring conformations and substituent orientations in these complexes. One can expect the six-membered ring to exist in a chair conformation; however, the seven-membered ring appears to be twisted such that it exists predominantly with one chiral sense relative to the phosphine.

Table IV. Temperature Dependence of Observed Chemical Shifts for [(η^2 -allyl)PdCl(PCoBF)]BF₄ (1)

T, °C	δ (H ₂)	δ (H ₁)	δ (H ₃)	δ (H ₅)	δ (H ₄)
30	34.6	31.4	25.9	24.8	22.3
25	35.7	32.5	26.5	25.3	22.9
10	38.1	34.7	28.1	26.9	24.2
-30	48.1	43.6	34.3	33.1	29.4
-50	55.1	49.8	38.6	37.4	32.9
-70	63.3	57.1	43.7	42.5	37.2

Reproducibility and Transferability of Chemical Shifts. Reference to Table I shows that the chemical shifts are dominated by the paramagnetic interaction with the PCoBF ligand. Furthermore, there is a relatively small range of shifts for a proton in a particular position; hence at a given temperature, the shift of a particular type of proton can be predicted empirically with good reliability. Small differences would be anticipated even on the basis of slight geometrical changes attending the substitution by methyl groups. From a practical point of view, however, once the position is established empirically from model compounds, it appears that the value can be transferred to other analogues with confidence.

We have assumed that the isotropic shifts induced in the allyl fragment are solely dipolar in nature and can be derived from the shift expression given in eq 3. Since these shifts derive from the magnetic susceptibility anisotropy of the Co(II), it follows that they should show a near-Curie dependence with temperature. As shown in Table IV the shifts increase dramatically upon lowering the temperature; hence, good temperature control is required for reproducibility. The temperature variation follows 1/T to give nearly straight-line plots, and the slopes allow a modest ability to predict crossovers and provide correlations with the diamagnetic PZnBF or triphenylphosphine complexes. The isotropic shift contribution to the observed chemical shift can be determined by comparison with zinc analogues of the PCoBF complexes as shown in Table I. These isotropic shifts, as well as relative slopes of shifts as obtained from plots of the data in Table IV, provide the most direct comparison with theoretical dipolar shift expressions. These data are useful if one actually attempts to compare shifts with calculated values of distances and angles from model complexes.

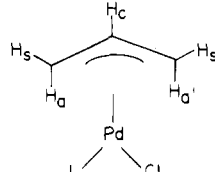
The isotropic shifts of the coordinated PCoBF ligand itself have components from both dipolar and contact terms; hence, the resonance observed at δ 23.8₅ at -50 °C moves downfield to δ 25.2₈ when the temperature is increased to 25 °C. These shifts appear to be consistent over a large number of complexes and provide a convenient internal calibration of the temperature.

The most convenient approach to correlations in the diamagnetic samples, however, is to plot the variation of shifts of all of the resonances relative to a resonance that can be assigned unequivocally and extrapolate back to the shifts observed in the diamagnetic complex. This method avoids temperature-control errors.

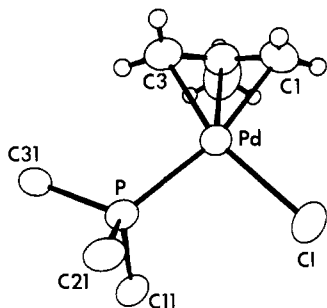
The charge on PCoBF or PZnBF modifies the trans effects of these phosphorus ligands relative to that of triphenylphosphine. Thus, although PPh₃ can be used to estimate shifts, some protons and H_a, in particular, show a large deviation. The values in Table V provide a basis for estimating corrections relative to triphenylphosphine. The extrapolated shifts must be used with considerable caution if used in making assignments. For example, the least-squares fit of shifts relative to the central proton shifts predicts values for H_a, H_{a'}, H_s, H_{s'}, and H_c, of δ 3.32, 5.17, 3.03, 6.01, and (6.28).

Correlations of NMR Data to Structure Using Models. Having empirically established the assignments of some methyl-substituted complexes (Table I) and noting that the shifts are fairly consistent among them (Figure 2), we wished to explore the potentiality of determining more detailed aspects of the geometry of the complexes.

Ideally one would like to compare the shifts with refined hydrogen positions in a PCoBF complex. Therefore, we initially attempted to determine the X-ray crystal structure of [(η^3 -2-methylallyl)PdCl(PCoBF)]BF₄ (2). Unfortunately we were unable

Table V. Chemical Shifts for Diamagnetic $[(\eta^3\text{-allyl})\text{PdCl}(\text{L})][\text{BF}_4]_n$ Complexes at -50°C in Acetone- d_6


proton	L = (PZnBF)	L = PPh ₃
H _a	3.69 ($J_{ac} = 12.2$ Hz)	3.11 ($J_{ac} = 12.0$ Hz)
H _{a'}	4.28 ($J_{pa'} \sim J_{ca'} \sim 11$ Hz)	3.66 ($J_{pa'} = 13.3$ Hz, $J_{ca'} = 9.8$ Hz)
H _s	4.67 ($J_{sc} = 6.7$ Hz)	3.01 ($J_{sc} = 6.9$ Hz)
H _{s'}	5.12 ($J_{ps'} \sim J_{s'c} \sim 7.5$ Hz)	4.51 ($J_{ps'} \sim J_{s'c} \sim 7.0$ Hz, $J_{ss'} = 1.9$ Hz)
H _c	6.28 (apparent septet)	5.79 (apparent septet)

**Figure 3.** ORTEP diagram showing 50% probability ellipsoids for the non-hydrogen atoms in $(\eta^3\text{-2-methylallyl})\text{Pd}(\text{PPh}_3)\text{Cl}$. The hydrogen atoms are shown in refined positions with B reduced to 1.0 \AA^2 , and only the ipso-carbon atoms of the phenyls are shown for clarity.

to obtain a crystal of high enough quality⁸ to afford accurate cobalt-hydrogen positions, although reliable Pd-P and Co-P lengths of 2.288 (5) and 3.407 (6) Å and a Co-P-Pd angle of $173.3 (2)^\circ$ were obtained. Also moderately precise Co-C(1), Co-C(2), and Co-C(3) distances of 7.81 (2), 7.23 (3), and 6.05 (2) Å were obtained. The allyl carbons refined with relatively high thermal parameters and larger uncertainties in bond lengths of C(1)-C(2) and C(2)-C(3) of 1.36 (3) and 1.49 (3) Å, suggesting considerable error in the calculation of idealized hydrogen positions. This structure of **2** with idealized hydrogen atom positions, however, provides a starting model to calculate shifts on the basis of eq 2.

A triphenylphosphine analogue appeared to be an attractive alternative for a reasonable model. Although a number of structures had been published, they did not provide sufficiently accurate data for our purposes and we therefore redetermined⁷ the structure of $[(\eta^3\text{-2-methylallyl})\text{PdCl}(\text{PPh}_3)]$ (**9**), including refinement of hydrogen atom positions. The essential features of the molecule are shown in Figure 3, and the other crystal data are given in the Experimental Section.

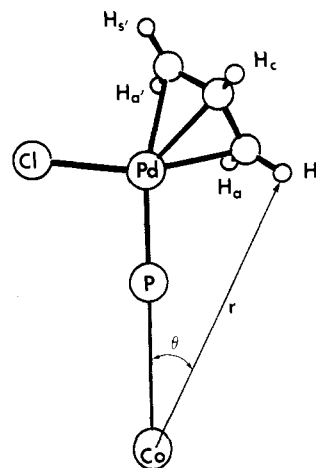
The positions of the carbon atoms should be accurately determined in this structure ($R_1 = 0.036$), and these provide the

(8) The crystals we obtained contained a disordered BF_4^- ion, as well as fractional solvent of crystallization which could not be refined successfully. The salt crystallizes in the monoclinic space group $P2_1/n$, with $a = 13.837 (4) \text{ \AA}$, $b = 13.489 (7) \text{ \AA}$, $c = 19.976 (7) \text{ \AA}$, and $\beta = 94.73 (3)^\circ$. Isotropic refinement of B, C, N, O and two half-occupied F atoms and anisotropic refinement of Pd, Co, P, Cl, and the remaining F atoms yielded final residuals of $R_1 = 0.105$ and $R_2 = 0.124$ for 1518 reflections with $F_o^2 \geq 3\sigma(F_o^2)$. The refinement converged to a structure expected for the complex, and the PCoBF portion was very similar to that found for the ligand itself, in which there was no disorder and $R_1 = 0.105$ (Churchill, M. R.; Reis, A. R. *J. Chem. Soc., Dalton Trans.* **1973**, 1570-1576). The final difference Fourier showed a number of peaks that were not in the vicinity of either the complex or the counterion, but these could not be successfully refined and identified with a particular conformation of solvent. Despite the disorders, the structure provided reasonably accurate parameters for the heavy atoms. The Pd-P and Co-P separations were respectively 2.288 (5) and 3.407 (6) Å with the Pd-P-Co angle being $173.3 (2)^\circ$.

Table VI. Calculated Isotropic Shifts Based on Geometrical Models

	obsd		calcd		
	1	2	X-ray 9	planar 9	planar 2
H _c	20.2		(20.2) ^a	(20.2)	(20.2)
H _{s'}	17.8	17.7	17.6	17.0	17.3
H _{a'}	21.0	21.2	21.8	24.6	26.3
H _a	28.8	28.3	28.3	39.7	50.6
H _s	31.0	29.9	36.1	31.5	34.0
Me _c		15.7	16.2		17.0

^a $D = 0.540 \times 10^{-26} \text{ cm}^3$ at 25°C is based on this value.

**Figure 4.** Distances and angles required for the dipolar shift equation (eq 2).

basis for another model, if one assumes the hydrogen atoms to lie in the allyl plane at idealized positions with C-H bond distances of 1.09 \AA .⁹ An early low-temperature X-ray determination designed to determine the H atom positions in allylpalladium chloride suggested that they lie in the plane;¹⁰ however, deviations of methyl groups from the plane in substituted allyls¹¹ suggest otherwise. Although the accuracy for the determination of H positions is somewhat lower than with heavier atoms, X-ray structures should provide reasonably reliable data for angles involving C-H bonds.¹² The structure determination of $(\eta^3\text{-2-methylallyl})\text{Pd}(\text{PPh}_3)\text{Cl}$ included refinement of the hydrogen atoms in the 2-methylallyl ligand as well as in the phenyl groups. The location of the hydrogen atoms at normal angles and distances in the phenyl groups suggests a reason for further confidence that the positions obtained in the 2-methylallyl ligand can be accepted as being fairly reliable. Therefore, we also developed a third model in which the positions were used as obtained from the crystal structure and were not lengthened to account for the shortening inherent in the X-ray determination of electron density, as opposed to nuclear position.

Both models based on **9** assume a P-Co vector colinear with the Pd-P bond with a P-Co distance of 3.40 Å. The central H position was taken as 1.09 \AA along the C(2)-C(4) vector. Since the magnetic susceptibility anisotropy was unknown, the D factor for eq 2 was calculated from the geometrical terms for the central hydrogen and the isotropic shift of 20.2 ppm at 25°C . Along with the r and θ values for the other protons in the models (Figure 4), one can predict the isotropic shifts shown in Table VI.

Except for the value for H_s, the values are matched well by using the positions determined by X-ray refinement of hydrogen positions

(9) Some of the most accurate C-H bond lengths for an η^3 -allyl appear to be those found in the low-temperature neutron diffraction structure of the $\text{Fe}[\text{P}(\text{OMe})_3][\text{C}_3\text{H}_3]^+$ cation (Brown, R. K.; Williams, J. M.; Schultz, A. J.; Stucky, G. D.; Ittel, S. D.; Harlow, R. L. *J. Am. Chem. Soc.* **1984**, *102*, 981-987); hence we have assigned a bond length of 1.09 \AA to the C-H bonds in the model.

(10) Smith, A. E. *Acta Crystallogr.* **1965**, *18*, 331-340.

(11) Mason, R.; Wheeler, A. G. *J. Chem. Soc. A* **1968**, 2543-2549.

(12) Churchill, M. R. *Inorg. Chem.* **1973**, *12*, 1213-1214. Teller, R. G.; Bau, R. *Struct. Bonding (Berlin)* **1981**, *44*, 1-82.

Table VII. Angles (α) Calculated from Quadrupole Splittings in the 76.8-MHz ^2H NMR Spectra at -25°C

	obsd $\Delta\nu_Q$, Hz (α_{calcd} , deg)		angles obtained from models, deg		
	1	2	X-ray 9	planar 9	planar 2
H_s'	18 (50)	<10 (52-57)	47	38	22
H_a'	67 (99, 81) ^a	59 (104, 76)	97	107	111
H_a	71 (94, 86) ^a	56 (106, 74)	86	105	112
H_s	<7 (147-143)	<7 (147-143)	137	121	123

^a Four solutions for α exist in eq 4 if the sign of $\Delta\nu_Q$ is not known. The values for the anti protons must be negative; however, this still leads to an ambiguity near 90° .

in **9**. Thus, the model based on the planar allyls in **9** or **2** would have reversed the assignments of H_s and H_a . The poor agreement with the planar allyl models suggests that the terminal hydrogen atoms are twisted from the plane.

Use of Quadrupolar Splittings in ^2H NMR Spectra. The value of the proportionality constant, D , in eq 2 increases with the lowering of temperature, as indicated by the increase in shifts. D is related to the magnetic susceptibility anisotropy for an axial case by eq 3.¹³ Thus, insofar as the models provide an accurate

$$D = -[\Delta\chi]/3 = -[\chi_{\parallel} - \chi_{\perp}]/3 \quad (3)$$

distance and angle from the cobalt to the central proton, the isotropic shift provides a reliable measure of D and, consequently, the value for the magnetic anisotropy. Anisotropic molecules orient to some degree in high magnetic fields, and this is expressed as a splitting of the ^2H resonances, which depends on the angle of the C-D bond relative to the axis of magnetic asymmetry (eq 4).

$$\Delta\nu_Q = \nu_Q^*(3 \cos^2 \alpha - 1) \quad (4)$$

ν_Q^* is a constant at a given temperature and depends upon a combination of orientational order parameters and magnetic susceptibility terms. This reduces to eq 5 for an axially symmetric

$$\nu_Q^* = [(e^2Qq/h)H_0/20kT][\chi_{\parallel} - \chi_{\perp}] \quad (5)$$

field gradient and axially symmetric magnetic susceptibility tensor.¹³ Thus, if one assumes a value of 165 kHz for the quadrupole coupling constant, e^2Qq/h , in these compounds,¹⁴ a value for ν_Q^* of 72.3 Hz is obtained at -25°C and one can predict the splittings for a given structural model or calculate the angles, α , for a given C-D bond (Table VII).

The functional form of eq 4 produces a wide variation of sensitivity of the splitting to angle. At 0 and 90° an uncertainty of $\pm 3^\circ$ only produces a variation in calculated splitting of ± 1 Hz, whereas at 45° there is a variation of ± 12 Hz. Likewise, the observed deviation from the predicted value of the splitting when $\alpha \sim 55^\circ$ is likely to be high.

Reference to Figure 4 qualitatively indicates that the carbon-anti deuterium bond vectors are nearly at right angles to the P-Co bond axis; hence, one would expect a large splitting in these deuteriums, and one would expect a fairly reliable prediction of the value of the splitting. Thus, for **2** $\Delta\nu_Q$ values for H_a' and H_s of 67 and 71 Hz are observed, and assuming an uncertainty of $\pm 3^\circ$, the X-ray model predicts values of -69 ± 1 and -71 ± 1 Hz. On the other hand, the syn protons are closer to the magic angle and $\Delta\nu_Q$ values for H_a' and H_a of 18 and <7 Hz are observed, and the X-ray model predicts values of 29 ± 11 and 45 ± 12 Hz. The predictions for the H_s proton are incorrect by a substantial margin, which was also true for the calculated isotropic shift. This particular position is also quite dependent on the model: when $\alpha(\text{H}_s) = 137^\circ$ in the X-ray model $\Delta\nu_Q = 45$ Hz, but when $\alpha(\text{H}_s) = 121^\circ$ in the planar model $\Delta\nu_Q = -14$ Hz.

The ultimate utility of quadrupole splittings will depend on the individual application. In this case it provides further evidence that the assignments were correct for H_a and H_s . This is important here because the assignments based on isotropic shifts would be reversed in the different models (Table V). The large splitting of the δ 28 resonance clearly indicates that it is the resonance for the anti proton.

The extraordinary sensitivity of the splittings to angle for some regions of α requires careful consideration of the error limits that can be expected. Thus, in some instances a difference of 20 Hz between predicted and observed splitting may be significant, and in others it may not be. Several other sources of error may also contribute significantly:

(1) The value of the quadrupole coupling constant may not be the same for each type of C-D bond; nevertheless, they should lie in the range 165-190 kHz.

(2) The Co-P and P-Pd vector are assumed to be colinear. In the accurately determined structure of (η^3 -2-methylallyl)Pd(PPh₃)Cl, the centroid of the three carbons attached to the phosphine is slightly displaced from the Pd-P vector. The Ct-P-Pd angle is 177.4° . In the crystal structure of the complex with PCoBF (**2**), the Co-P-Pd angle is 173.3 (2) $^\circ$, which can account for significant deviations between the calculated and observed values for models based on **9**. Reference to Tables VI and VII provides an indication of the importance of this deviation in angle. In practice, however, one is often forced to use idealized models in the absence of sufficiently accurate crystallographic data. Our purpose here was to demonstrate the predictability in the more common situation where detailed structural data were not available.

(3) Reproducible temperatures are required, as the quadrupole splittings have a $1/T^2$ dependence.

Line Width Dependence on Geometry. Line widths generally increase with greater isotropic shift. Thus for **1**, one sees half-widths of 382, 270, 135, 124, and 90 Hz at -70°C in the ^1H NMR spectrum from the most shifted to the least shifted resonances. These widths can sometimes be used as a further confirmation of assignment, owing to their relationship to distance and angle parameters.^{15,16} If the magnetic susceptibility were isotropic, the relative line widths would be proportional to $1/r^6$, where r is the distance from the proton to the paramagnetic center. Consequently, a crude estimate for the relative line widths can be made by using the $1/r^6$ dependence. Thus, the ratio of the line widths, W_i/W_j , is roughly proportional to r_j^6/r_i^6 .¹⁵ For anisotropic axially symmetric systems like that in PCoBF, there is a substantial additional term depending on $(\cos^2 \theta)/r^6$.¹⁶ Consequently, this term tends to reduce the line width for a given r^6 as θ increases from 0 to 90° .

With larger values of θ , the $(3 \cos^2 \theta - 1)$ term can reduce the isotropic shift, such that a nucleus with a relatively small r may not have as large a shift as expected qualitatively. The interplay of the relative importance of r^{-3} and r^{-6} and the $(3 \cos^2 \theta - 1)$ and the $\cos^2 \theta$ dependences can produce situations in which the larger isotropic shifts are not necessarily associated with the larger line widths. This situation is observed in the 1,3-dimethylallyl complex (**5**), where the cis syn methyl group at δ 34.0 has a half-width of 283 Hz, whereas the cis anti proton at δ 49.1 only has a half-width of 182 Hz. The anti proton has $\theta \sim 26^\circ$, whereas the average methyl proton θ is $\sim 35^\circ$.¹⁷ r for the anti proton is ~ 6.8 Å, and the average r for the methyl protons is ~ 6.2 Å. Thus, the methyl protons are closer, but have a smaller isotropic shift owing to the $(3 \cos^2 \theta - 1)$ dependence. The r^{-6} dependence, however, dominates the relaxation and produces a broader resonance.

Distortions of Allyl Ligands. The X-ray determination of the structure of **9** clearly shows that the hydrogen atoms are displaced

(13) Domaille, P. J. *J. Am. Chem. Soc.* **1980**, *102*, 5392-5393. We assume here that the field gradients for all of the C-D bonds are the same.

(14) Coupling constants for sp^3 and sp^2 hybridization at carbon are ~ 165 and ~ 185 kHz, respectively, in model organic compounds (Mantsch, H. M.; Saito, H.; Smith, I. C. P. *Prog. Nucl. Magn. Reson. Spectrosc.* **1977**, *11*, 211-271). The effect that the binding to a metal may have is unclear.

(15) LaMar, G. N.; Faller, J. W. *J. Am. Chem. Soc.* **1973**, *95*, 3817-3818.

(16) LaMar, G. N.; Metz, E. A. *J. Am. Chem. Soc.* **1974**, *96*, 5611-5612. Sternlicht, H. *J. Chem. Phys.* **1965**, *42*, 2250-2251.

(17) In calculations of averages, one should note that $\langle r \rangle^6$ is not the same as $\langle r^6 \rangle$. A similar situation holds in averages of θ , $\cos \theta$ and $\cos^2 \theta$.

from the plane of the carbon atoms of the allyl. The deviations from the plane were large (see Experimental Section) and were substantially greater than any deviations found with the phenyl hydrogen atoms from the plane of the phenyl groups. Reference to Figure 3 shows that the syn protons twist toward the metal and the anti protons twist away. The methyl group also bends toward the metal. The bending of the methyl in η^3 -methylallyl complexes has been noted in a number of previous cases.¹⁸⁻²² Deviations of this type can be ascribed to mixing of the π and σ orbitals in the allyl ligand.²³ The degree of bending has also been related to the effective charge on the allyl,²⁴ and the distortions in a number of complexes have been reviewed and discussed recently.²⁴ Although the distortions can be attributed to electrostatic effects in alkali-metal complexes, an attractive qualitative explanation from our point of view is that the σ framework of the allyl twists and rehybridizes to maximize the overlap of the p orbitals of the allyl with the d orbitals of the metal.

The near equality of the C(1)–C(2) and C(2)–C(3) bonds of the allyl in **9** is another feature of the structure deserving some comment. The π – σ – π rearrangement of allyl groups had been well documented,⁶ and several crystal structure determinations in the late 1960s suggested that the difference in trans effects in unsymmetrical complexes, such as **9**, could be attributed to partial conversion to a π – σ type of bonding in the ground state.^{7,25} Significant differences in carbon–carbon bond lengths were originally found in both the allyl²⁵ and 2-methylallyl⁷ ligands attached to PdCl(PPh₃). Subsequent study of the room-temperature structure of the (allyl)PdCl(PPh₃) indicated that the C–C lengths were nearly the same,²⁶ and the structure reported in this current paper also shows that this is true in the 2-methylallyl complex. A structure with a thioacetylacetonate-type ligand also showed nearly equal C–C lengths.²⁷ Hence, although it is clear that the ligands trans to a Pd–C bond can drastically alter its length, it appears that the change in the allyl C–C bond is not significant.

Experimental Section

Reagent grade solvents were used as supplied by the manufacturer. Deuterated NMR solvents were stored over molecular sieves. Elemental analyses were performed by Galbraith Laboratories, Knoxville, TN. All NMR spectra were obtained on a Bruker HX270 instrument, a 270-MHz spectrometer. The [fluoro(2,2',2''-phosphinidynetris(pyridine-carbaldoximato))borato]cobalt(II) and zinc(II) tetrafluoroborate complexes and the allylpalladium chloride dimers were synthesized from allyl chlorides and PdCl₂ via published procedures.^{4,6,28-30}

Syntheses. The preparation of all of the [(allyl)PdCl(PMBF)]BF₄ (M = Co, Zn) complexes followed procedures analogous to those given in the example below.

[(η^3 -2-methylallyl)PdCl(PCoBF)]BF₄ (**2**). The clathrochelate ligand PCoBF⁺BF₄[−] (118 mg, 0.209 mmol) and [(η^3 -2-methylallyl)PdCl]₂ (40 mg, 0.104 mmol) were combined in acetonitrile (4 mL). Formation of a yellow crystalline solid began after the solution was stirred for 5 min. The solution was stirred for 1 h at room temperature, and diethyl ether (4 mL) was added. The yellow solid was filtered, washed with diethyl ether, and dried in vacuo to yield 139 mg of the product (88%). Additional product could be obtained by the addition of more ether. The

Table VIII. Crystallographic Data for X-ray Diffraction Studies of [(η^3 -2-CH₃C₃H₄)]Pd(PPh₃)Cl

(A) Crystal Data	
formula	PdClPC ₂₂ H ₂₂
temp, °C	24 ± 3
space group	P2 ₁ /c (No. 14)
a, Å	11.931 (4)
b, Å	9.783 (2)
c, Å	17.286 (6)
β , deg	97.40 (3)
V, Å ³	2000.9 (1.8)
M _r	459.25
ρ_{calcd} , g/cm ³	1.52
Z	4
(B) Measurement of Intensity Data	
radiation	Mo K α (0.71073 Å)
monochromator	graphite
detector aperture, mm	
horizontal (A + B tan θ)	3.0, 1.0
vertical	4.0
reflens measd	+h, +k, \pm l
max 2 θ , deg	50
scan type	moving cryst–stationary counter
ω scan width (A + 0.347 tan θ), deg	
A	1.20
bkgd	1/4 additional at each end of scan
ω scan rate (variable)	
max, deg/min	10.0
min, deg/min	1.7
no. of reflens measd	3923 including absences
no. of data used [$F^2 \geq 3\sigma(F^2)$]	2219
(C) Treatment of Data	
abs cor	not applied
abs coeff, cm ^{−1}	11.3
p factor	0.03
final residuals	
R ₁	0.036
R ₂	0.040
esd of unit weight	1.54
largest shift/error value on final cycle	0.01
largest peak in final difference Fourier, e/Å ²	0.31

complex was recrystallized from 1:1 acetonitrile/ether.

Anal. Calcd for C₂₂H₁₉PdClB₂F₅N₆O₃CoP: C, 34.76; H, 2.52; N, 11.05. Found: C, 34.45; H, 2.88; N, 11.29.

The other [(allyl)PdCl(PCoBF)]BF₄ complexes were prepared by using the appropriate allylpalladium dimer. The product did not precipitate from the reaction mixture in some cases, but crystallization could be induced by the addition of more ether. The preparations of [(η^3 -allyl)PdCl(PCoBF)]BF₄ (**1**) and [(η^3 -1,1-dimethylallyl)PdCl(PCoP)]BF₄ (**4**) were carried out in 1:1 acetone/acetonitrile. Yields ranged from 85 to 100%.

Deuterated Allyl Alcohols. We found the best method for the deuterium labeling of allylic alcohols at the allylic position to be reduction of the corresponding acid chloride by lithium aluminum deuteride, as described by Schuetz and Millard.³¹ Each molecule of LiAlD₄ was assumed to contain two active deuterides, thus requiring 1 mol of LiAlD₄/mole of acid chloride. Procedures similar to that below were used for all alcohols.

CH₃CHCD₂OH. The reaction flask was charged with 5.56 g of LiAlD₄ (0.132 mol) and 250 mL of dry Et₂O. The resulting water-white slurry was then chilled to \sim −10 °C with an ice/water/NaCl bath and treated dropwise, with stirring, with 10.0 mL of acryloyl chloride (0.123 mol) in 50 mL of dry ether from an addition funnel. The vigorous exothermic reaction was moderated by controlling the rate of addition such that the temperature of the reaction mixture did not rise above +5 °C. Typically, the addition took \sim 1.5 h to complete, after which time the reaction mixture was allowed to warm to room temperature and stir for an additional 2 h. The mixture was then recharged with an ice bath and hydrolyzed. The hydrolysis followed the procedure recommended

- (18) Uttech, R.; Dietrich, H. Z. *Kristallogr., Kristallgeom., Kristallphys., Kristallchem.* **1965**, *122*, 60.
 (19) Helmholtz, R. B.; Jellinek, F.; Martin, H. A.; Vos, A. *Recl. Trav. Chim. Pays-Bas* **1967**, *86*, 1263.
 (20) Churchill, M. R.; O'Brien, T. A. *Chem. Commun.* **1968**, 246–247.
 (21) Mason, R.; Wheeler, A. G. *Nature (London)* **1968**, *217*, 1253.
 (22) Lippard, S. J.; Morehouse, S. M. *J. Am. Chem. Soc.* **1969**, *91*, 2504.
 (23) Kettle, S. F. A. *Inorg. Chim. Acta* **1967**, *1*, 303. Kettle, S. F. A.; Mason, R. *J. Organomet. Chem.* **1966**, *5*, 573.
 (24) (a) Kaduk, J. A.; Poulos, A. T.; Ibers, J. A. *J. Organomet. Chem.* **1977**, *127*, 245–260. (b) Clark, T.; Rohde, C.; Schleyer, P. *Organometallics* **1983**, *2*, 1344–1351. (c) Henc, B.; Jolly, P. W.; Salz, R.; Stobbe, S.; Wilke, G.; Benn, R.; Mynott, R.; Seevogel, K.; Goddard, R.; Krueger, C. *J. Organomet. Chem.* **1980**, *191*, 449. (d) Decher, G.; Boche, G. *J. Organomet. Chem.* **1983**, *259*, 31–36.
 (25) Low-temperature structure: Smith, A. E. *Acta Crystallogr., Sect. A: Cryst. Phys., Diff., Theor. Gen. Crystallogr.* **1964**, *25*, S161.
 (26) Smith, A. E., private communication quoted by S. J. Lippard.²⁷
 (27) Lippard, S. J.; Morehouse, S. M. *J. Am. Chem. Soc.* **1972**, *94*, 6956.
 (28) Dent, W. T.; Long, R.; Wilkinson, A. J. *J. Chem. Soc.* **1964**, 1585.
 (29) Tatsuno, Y.; Yoshida, T.; Otsuka, S. *Inorg. Synth.* **1979**, *19*, 220.
 (30) Trost, B. M.; Stregge, P. E.; Weber, L.; Fullerton, T. J.; Dietsche, T. J. *J. Am. Chem. Soc.* **1978**, *100*, 3407.

- (31) Schuetz, R. D.; Millard, F. W. *J. Org. Chem.* **1959**, *24*, 297–300; McMichael, K. D. *J. Am. Chem. Soc.* **1967**, *89*, 2943–2947. Kim, J. K.; Caserio, M. C. *J. Org. Chem.* **1979**, *44*, 1897–1904.

Table IX. Positional and Thermal Parameters for (η^3 -2-methylallyl)PdCl(PPh₃)

atom	<i>x/a</i>	<i>y/b</i>	<i>z/c</i>	<i>B</i> _{eqv} , Å ²
Pd	0.17533 (4)	0.03368 (5)	0.03785 (2)	2.932 (8)
Cl	0.1733 (1)	0.1036 (2)	0.16959 (9)	4.65 (4)
P	0.2696 (1)	-0.1700 (2)	0.06521 (8)	2.87 (3)
C(1)	0.0757 (5)	0.2071 (6)	-0.0165 (4)	4.1 (1)
C(2)	0.1532 (5)	0.1647 (6)	-0.0638 (3)	4.0 (1)
C(3)	0.1493 (5)	0.0273 (7)	-0.0858 (3)	4.3 (1)
C(4)	0.2486 (6)	0.2561 (8)	-0.0787 (4)	6.5 (2)
C(11)	0.4013 (4)	-0.1420 (6)	0.1274 (3)	3.0 (1)
C(12)	0.4562 (5)	-0.0188 (7)	0.1224 (3)	4.0 (1)
C(13)	0.5588 (5)	0.0062 (7)	0.1682 (4)	4.8 (2)
C(14)	0.6053 (5)	-0.0898 (8)	0.2171 (4)	5.0 (2)
C(15)	0.5537 (5)	-0.2129 (7)	0.2238 (3)	4.6 (2)
C(16)	0.4520 (5)	-0.2397 (7)	0.1786 (3)	3.8 (1)
C(21)	0.1940 (4)	-0.2962 (6)	0.1169 (3)	3.1 (1)
C(22)	0.1285 (5)	-0.2521 (7)	0.1716 (3)	4.2 (1)
C(23)	0.0703 (6)	-0.3428 (7)	0.2125 (4)	5.4 (2)
C(24)	0.0751 (6)	-0.4766 (8)	0.1983 (4)	5.4 (2)
C(25)	0.1386 (6)	-0.5244 (7)	0.1447 (4)	5.5 (2)
C(26)	0.1994 (5)	-0.4347 (6)	0.1026 (4)	4.3 (2)
C(31)	0.3094 (4)	-0.2671 (6)	-0.0168 (3)	3.0 (1)
C(32)	0.2250 (5)	-0.3083 (7)	-0.0761 (3)	4.2 (1)
C(33)	0.2530 (6)	-0.3817 (7)	-0.1385 (3)	5.1 (2)
C(34)	0.3608 (6)	-0.4152 (7)	-0.1448 (4)	5.2 (2)
C(35)	0.4435 (6)	-0.3779 (8)	-0.0879 (4)	5.4 (2)
C(36)	0.4197 (5)	-0.3026 (7)	-0.0238 (3)	4.2 (1)
H(12)	0.428 (4)	0.046 (4)	0.088 (2)	2 (1)
H(13)	0.586 (4)	0.084 (5)	0.159 (3)	4 (1)
H(14)	0.674 (4)	-0.079 (5)	0.245 (3)	4 (1)
H(15)	0.585 (4)	-0.280 (5)	0.261 (3)	4 (1)
H(16)	0.412 (4)	-0.327 (5)	0.177 (3)	3 (1)
H(22)	0.114 (4)	-0.157 (6)	0.178 (3)	5 (1)
H(23)	0.016 (6)	-0.290 (8)	0.256 (4)	8 (2)
H(24)	0.040 (5)	-0.537 (6)	0.225 (3)	5 (1)
H(25)	0.148 (4)	-0.600 (5)	0.140 (3)	4 (1)
H(26)	0.252 (4)	-0.475 (5)	0.068 (3)	3 (1)
H(32)	0.162 (4)	-0.275 (5)	-0.076 (3)	4 (1)
H(33)	0.201 (4)	-0.399 (6)	-0.172 (3)	5 (1)
H(35)	0.525 (5)	-0.392 (6)	-0.085 (3)	7 (2)
H(36)	0.474 (4)	-0.266 (5)	0.016 (3)	4 (1)
H(1s)	0.080 (4)	0.293 (5)	0.008 (3)	4 (1)
H(1a)	0.020 (4)	0.158 (5)	-0.018 (3)	3 (1)
H(3a)	0.075 (6)	-0.015 (7)	-0.100 (4)	8 (2)
H(3s)	0.209 (4)	-0.024 (5)	-0.106 (3)	4 (1)
H(41)	0.236 (5)	0.296 (7)	-0.124 (4)	8 (2)
H(42)	0.316 (6)	0.210 (7)	-0.087 (4)	9 (2)
H(43)	0.264 (4)	0.319 (5)	-0.040 (3)	4 (1)

by Gaylord³² and used successive dropwise addition of 6 mL of water, 4 mL of 20% NaOH, and 19 mL of water. During the hydrolysis, the contents of the flask were stirred and care was taken to allow for the escape of H₂ by means of an efficient oil bubbler. The reaction mixture was typically allowed to stir at room temperature overnight. This aided in the formation of a granular white precipitate of lithium salts, which allowed for the facile separation of the ether solution by decantation. The lithium salts were washed several times with small amounts of ether, and the washes were combined with the decantate and dried over Na₂SO₄. The ether was removed from the product by careful distillation to avoid overheating the pot. The remaining colorless liquid (~8 mL) was assayed by ¹H NMR and found to contain a mixture of the desired deuterated allyl alcohol and some undistilled ether in ~4:1 molar ratio, i.e. a yield of 5.9 g (~80%). This crude deuterated alcohol was judged to be of sufficient purity for conversion to the allylic chloride. (Attempts to distill the alcohol at elevated temperatures leads to polymerization.) The ¹H NMR spectrum was in good agreement with the data reported by McMichael.³¹ In particular, the absence of the doublet at δ 4.00 for the α -methylene protons and the simplification of the 10-line multiplet of the β -vinyl proton were evidence of a highly selective deuteration.

Deuterated Allyl Chlorides. Of the numerous synthetic methods for converting allylic alcohols to allylic chlorides, the procedure described by Magid et al.³³ was found to be superior for the low-boiling allylic chlorides need in this work. This reaction involves the reagent system

Table X. Selected Bond Distances (Å) for (η^3 -2-methylallyl)PdCl(PPh₃)

Pd-Cl	2.381 (1)	C(1)-H(1s)	0.94 (5)
Pd-P	2.307 (1)	C(1)-H(1a)	0.82 (5)
Pd-C(1)	2.211 (6)	C(2)-C(3)	1.396 (8)
Pd-C(2)	2.163 (5)	C(2)-C(4)	1.496 (9)
Pd-C(3)	2.120 (5)	C(3)-H(3a)	0.99 (6)
P-C(11)	1.807 (5)	C(3)-H(3s)	0.97 (5)
P-C(21)	1.829 (5)	C(4)-H(41)	0.88 (7)
P-C(31)	1.821 (5)	C(4)-H(42)	0.95 (7)
C(1)-C(2)	1.374 (8)	C(4)-H(43)	0.91 (5)

Table XI. Selected Bond Angles (deg) for (η^3 -2-methylallyl)PdCl(PPh₃)

Cl-Pd-P	96.70 (5)	C(2)-C(1)-H(1s)	123 (3)
Cl-Pd-C(1)	96.6 (2)	C(2)-C(1)-H(1a)	114 (4)
Cl-Pd-C(2)	126.3 (2)	H(1s)-C(1)-H(1a)	122 (5)
Cl-Pd-C(3)	162.6 (2)	C(1)-C(2)-C(3)	116.9 (6)
P-Pd-C(1)	166.2 (2)	Pd-C(3)-H(3a)	106 (4)
P-Pd-C(2)	133.1 (2)	Pd-C(3)-H(3s)	111 (3)
P-Pd-C(3)	100.7 (2)	C(2)-C(3)-H(3a)	118 (4)
Pd-P-C(11)	110.8 (2)	C(2)-C(3)-H(3s)	126 (3)
Pd-P-C(21)	115.2 (2)	H(3a)-C(3)-H(3s)	112 (5)
Pd-P-C(31)	117.4 (2)	C(2)-C(4)-H(41)	112 (5)
C(11)-P-C(21)	104.9 (2)	C(2)-C(4)-H(42)	115 (5)
C(11)-P-C(31)	104.4 (2)	C(2)C(4)-H(43)	111 (3)
C(21)-P-C(31)	102.9 (2)	H(41)-C(4)-H(42)	97 (6)
Pd-C(1)-H(1s)	120 (3)	H(41)-C(4)-H(43)	110 (6)
Pd-C(1)-H(1a)	87 (4)	H(42)-C(4)-H(43)	110 (6)

hexachloroacetone (HCA)/triphenylphosphine and is advantageous in that it is rapid and mild (no allylic rearrangement) and the products can be distilled directly from the reaction mixture with little or no contamination from byproducts.

CH₂CHCD₂Cl. Reactions were carried out in 50-mL Schlenk flasks under an atmosphere of dry nitrogen. HCA served as the solvent and was present in excess. A 10% excess of PPh₃ was also employed. The flask containing a Teflon-coated magnetic stirbar was charged with 9.5 g of PPh₃ (36 mmol) and 20 mL of HCA. The resulting slurry was chilled to 0 °C and, with vigorous stirring, was treated dropwise with 2.0 g of allyl-*l,l*-d₂ alcohol (33 mmol), which was added via a stainless-steel transfer needle. An exothermic reaction occurred immediately. The PPh₃ slowly went into solution, and the reaction mixture gradually darkened. After the addition was completed, the ice bath was removed and the reaction mixture allowed to stir for 0.5 h. During this time a thick slurry formed owing to precipitation of insoluble Ph₃PO. The product was isolated by distilling it directly from the reaction mixture (bp 46–47 °C); (or under vacuum for higher boiling halides). The allylic chloride prepared by this method was obtained in 90% yield and was contaminated only by Et₂O carried over from the preparation of the precursor alcohol. The ¹H NMR spectrum of the halide was virtually identical with that of the alcohol except for the absence of the OH signal.

Crystallographic Analyses. Crystals suitable for diffraction analysis were obtained from dichloromethane/hexane solutions by cooling to -10 °C. A crystal was mounted in a thin-walled glass capillary. Diffraction measurements were carried out on an Enraf-Nonius CAD-4 fully automated four-circle diffractometer. Unit cells were determined and refined from 25 randomly selected reflections obtained by using the CAD-4 automatic search, center, index, and least-squares routines. The crystal data and the data collection parameters are listed in Table VIII. Data processing was performed on Digital PDP 11/45 and 11/23 computers with the Enraf-Nonius SDP program library (Version 18). Absorption corrections were not performed owing to the low absorption coefficients. Neutral-atom scattering factors were calculated by standard procedures.^{34a} Anomalous dispersion corrections were applied to all atoms.^{34b} Full-matrix least-squares refinements minimized the function $\sum_{hkl} w(|F_o| - |F_c|)^2$, where $w = 1/\sigma(F)^2$, $\sigma(F) = \sigma(F_o^2)/2F_o$, and $\sigma(F_o^2) = [\sigma(I_{raw})^2 + (PF_o^2)^2]^{1/2}/Lp$.

The space group *P*2₁/*c* was established by the systematic absences for 9. The structure was solved by a combination of Patterson and difference Fourier techniques.

Anisotropic refinement of all non-hydrogen atoms and analysis of subsequent difference Fourier maps revealed all of the hydrogen atoms.

(32) Gaylord, N. G. "Reduction with Complex Metal Hydrides"; Interscience: New York, 1956; pp 391, 1007.

(33) Magid, R. M.; Fruchey, O. S.; Johnson, W. L.; Allen, T. G. *J. Org. Chem.* 1979, 44, 359–363.

(34) "International Tables for X-ray Crystallography"; Kynoch Press: Birmingham, England, 1975; Vol. IV: (a) Table 2.2B, pp 99–101; (b) Table 2.3.1, pp 149–150.

Table XII. Unit-Weighted Least-Squares Planes for (η^3 -2-methylallyl)PdCl(PPh₃)

plane	atoms	dist from plane, Å
1	C(1), C(2), C(3)	0.00
	C(4)	-0.230 (7)
	Pd	-1.717 (1)
	H(1s)	-0.15 (5)
	H(1a)	0.27 (5)
	H(3a)	0.58 (7)
	H(3s)	-0.25 (5)
	2	C(1), H(1s), H(1a)
3	C(3), H(3s), H(3a)	0.00
4	C(2), C(1), H(1s)	0.00
5	C(2), C(1), H(1a)	0.00
6	C(2), C(3), H(3a)	0.00
7	C(2), C(3), H(3s)	0.00

planes	dihedral angle, deg	planes	dihedral angle, deg
1-2	20	1-5	22
1-3	36	1-6	42
1-4	11	1-7	19

The hydrogen atoms were included and refined to converge to the residuals and parameters given in Table VIII. The values of the fractional coordinates are listed in Table IX. Selected bond lengths and angles and the esd's obtained from the inverse matrix obtained on the final cycle of refinement are given in Tables X and XI. Least-squares planes are given

in Table XII. Tables of anisotropic thermal parameters, structure factor amplitudes, and phenyl parameters are available in the supplementary material.

The disordered solvent and anion in the crystal of **2** prevented a satisfactory solution of the structure for use in accurate bond length determinations. We hope that a satisfactory crystal may be obtained with other counterions in the future. The coordinates for this structure are also included in the supplementary material.

Acknowledgment. We wish to thank the NSF for support of this research.

Registry No. **1**, 99232-27-6; **2**, 99212-69-8; **3**, 99212-71-2; **4**, 99212-73-4; **5**, 99232-29-8; **6a**, 99212-75-6; **6b**, 99266-43-0; **7**, 99232-31-2; **8**, 99232-33-4; **9**, 12098-21-4; PCoBF⁺BF₄⁻, 34323-77-8; PZnBF⁺BF₄⁻, 28042-05-9; CH₂CHCD₂OH, 10475-51-1; CH₂CHCD₂Cl, 37730-14-6; [(η^3 -allyl)PdCl(PPh₃)], 12097-84-6; [(η^3 -allyl)PdCl-(PZnBF)] [BF₄], 99212-77-8; [(η^3 -allyl)PdCl]₂, 12012-95-2; [(η^3 -2-methylallyl)PdCl]₂, 12081-18-4; [(η^3 -1-methylallyl)PdCl]₂, 12081-22-0; [(η^3 -1,1-dimethylallyl)PdCl]₂, 12288-41-4; [(η^3 -1,3-dimethylallyl)PdCl]₂, 12245-05-5; [(η^3 -1-acetyl-2-methylallyl)PdCl]₂ (isomer 1), 31832-96-9; [(η^3 -1-acetyl-2-methylallyl)PdCl]₂ (isomer 2), 31869-20-2; [(η^3 -cyclohexenyl)PdCl]₂, 12090-09-4; [(η^3 -cycloheptenyl)PdCl]₂, 35284-32-3.

Supplementary Material Available: Tables of calculated and observed structure factor amplitudes, anisotropic thermal parameters (B_{ij} 's), selected phenyl bond angles for (2-methylallyl)PdCl(PPh₃), and positional and thermal parameters for (2-methylallyl)PdCl(PCoBF) (14 pages). Ordering information is given on any current masthead page.

Contribution from the University Chemical Laboratory,
Cambridge CB2 1EW, U.K.

Ligand-Field Parameters and the Stereochemical Activity of d Shells in Trigonal-Bipyramidal Complexes of the First Transition Series[†]

R. J. Deeth and M. Gerloch*

Received March 1, 1985

Angular-overlap-model analyses of the trigonal-bipyramidal (TBP) complexes [M(Me₆tren)Br]Br (M = Cr, Fe, Co, Ni, Cu; Me₆tren = tris(dimethylamino)ethylamine) and for [Cu(tren)NH₃](ClO₄)₂ (tren = tris(aminoethyl)amine) are reported. Changes in the ligand-field parameters and detailed bond length variations throughout the complete Me₆tren series chromium to zinc describe a situation dominated by the variable dⁿ configuration. The possibility that the relatively low ligand-field strengths of the equatorial ligands in TBP complexes of copper(II) may arise from (negative) contributions by in-plane coordination voids rather than from the stereochemical activity of the d⁹ shell is shown to be untenable.

Introduction

Ligand-field analyses¹ of [Cu(bpy)₂I]I and [Cu(phen)₂H₂O](NO₃)₂ (bpy = 2,2'-bipyridyl; phen = 1,10-phenanthroline), have established markedly greater axial than equatorial angular-overlap-model (AOM) parameter values for these unsaturated chelates despite closely similar copper-nitrogen bond lengths. There is obviously no simple relationship between bond length and the magnitude of ligand-field parameters in these systems: in fact, the asymmetric chelation from these ligands arises from the stereochemical activity of the incomplete d shell.

More detailed comparisons between the AOM parameters for these two complexes center on the role of coordination voids, which have been shown² to be important in tetragonal copper(II) systems. We have argued that the low e_g value for the equatorial water ligand in the phen complex reflects a significant, negative ligand-field contribution from the partially void region opposite. In this molecule the N_{eq}-Cu-N_{eq} angle is 140° whereas for the bpy complex it is 114°. The negative ligand field of a coordination void arises, not from empty space, but from that portion of metal s electron density that is essentially not preempted by bonding to adjacent ligands.^{3,4} The ligand-field role of a void cell will thus be determined in large measure by the angle subtended by

the neighboring ligands, and we expect that the quantitative contribution will vary with this geometrical feature in a strongly nonlinear way. In the phen complex, the 140° angle defines a region that is apparently large enough to exert a noticeable effect. Although we do not envisage a significant void contribution in the bpy complex, one *could* argue that the large difference between the AOM parameter values for the axial and equatorial sites in these TBP systems is due solely to the 120° angles subtended opposite the equatorial ligands. We have therefore sought systems for which ligand-field analyses can resolve this issue with clarity. The present study describes analyses for the complexes [M-(Me₆tren)Br]Br (M^{II} = Cr, Mn, Co, Ni, Cu, Zn; Me₆tren = tris(dimethylamino)ethylamine), which comprise a series of isomorphous TBP molecules. The closely related compound [Cu(tren)NH₃](ClO₄)₂, tren = tris(aminoethyl)amine, offers further opportunity for comparison (Figure 1).

Fitting

The ligand-field analyses described here are based upon the angular-overlap model as reformulated by Gerloch and Woolley.³⁻⁶ All

- (1) Deeth, R. J.; Gerloch, M. *Inorg. Chem.* **1984**, *23*, 3853.
- (2) Deeth, R. J.; Gerloch, M. *Inorg. Chem.* **1984**, *23*, 3846.
- (3) Gerloch, M.; Woolley, R. G. *Prog. Inorg. Chem.* **1984**, *31*, 371.
- (4) Gerloch, M. "Magnetism and Ligand-Field Analysis"; Cambridge University Press: Cambridge, 1983.

[†]No reprints available from this laboratory.